

Charge and energy dynamics in photo-excited poly(para-phenylenevinylene) systems

L. Gisslén,^{a)} Å. Johansson,^{b)} and S. Stafström^{c)}

Department of Physics, IFM Linköping University, SE-581 83 Linköping, Sweden

(Received 12 February 2004; accepted 23 April 2004)

We report results from simulations of charge and energy dynamics in poly(para-phenylenevinylene) (PPV) and PPV interacting with C₆₀. The simulations were performed by solving the time-dependent Schrödinger equation and the lattice equation of motion simultaneously and nonadiabatically. The electronic system and the coupling of the electrons to the lattice were described by an extended three-dimensional version of the Su-Schrieffer-Heeger model, which also included an external electric field. Electron and lattice dynamics following electronic excitations at different energies have been simulated. The effect of additional lattice energy was also included in the simulations. Our results show that both exciton diffusion and transitions from high to lower lying excitations are stimulated by increasing the lattice energy. Also field induced charge separation occurs faster if the lattice energy is increased. This separation process is highly nonadiabatic and involves a significant rearrangement of the electron distribution. In the case of PPV coupled to C₆₀, we observe a spontaneous charge separation. The separation time is in this case limited by the local concentration of C₆₀ molecules close to the PPV chain. © 2004 American Institute of Physics. [DOI: 10.1063/1.1763145]

I. INTRODUCTION

Organic polymers possess the ability to convert electrical energy into photon energy and vice versa.¹ In combinations with the potentially high conducting properties they constitute an excellent platform for many applications such as organic light emitting diodes² (OLED) and solar cells.^{3,4} While the OLEDs have already entered the market, organic solar cells still have a power conversion efficiency that is too low compared to the inorganic devices.⁵ This is partly due to low intrinsic charge carrier mobilities which leads to current losses via recombinations. To increase the efficiency of this type of device it is necessary to perform more profound studies of the processes that limit the power conversion. These processes include exciton generation and relaxation, charge separation, and charge transport. Here we study at all these processes, but most emphasis is put on the exciton relaxation and charge separation, where the latter is strongly dependent on the first. It turns out that highly excited electron-hole pairs are much easier to separate than the lower lying excitations. We have also studied the effect of adding lattice energy to the system, to simulate the effect an increased temperature can have on charge separation.

Two ways to achieve charge separation have been simulated here, by applying an external electrical field to poly(para-phenylenevinylene) (PPV) or by using the internal electric field build up in a donor/acceptor complex. It is well known from combined experimental and theoretical studies that the lowest excited state in PPV (as well as in many other conjugated polymers) is a polaron exciton, i.e., a bound

electron-hole pair dressed by a deformation of the lattice.⁶ Time resolved studies of field-induced dissociation of the polaron exciton have been performed in order to get information about, e.g., the binding energy of the exciton. In particular, it has been shown that the field-induced dissociation is ultrafast and leads to the creation of a pair of oppositely charged polarons on separate chains.⁷⁻¹⁰ Sariciftci *et al.*³ found a similar type of ultrafast exciton dissociation in a PPV/C₆₀ system upon excitation of PPV. In this case, the dissociation occurs spontaneously, without an external electric field. The excited electron is transferred into the lowest unoccupied molecular orbital (LUMO) level of C₆₀, a process which is found to occur at a sub-picosecond time scale.¹¹⁻¹³

The initial phase of charge transport following electron-hole separation is included in our simulations. This initial phase involves intrachain polaron drift or electron hopping between C₆₀ molecules. More extensive studies of intermolecular transport processes were reported previously¹⁴ and will be discussed in connection with the results obtained in this study.

The paper is organized as follows. The methodology is introduced in Sec. II and results are presented and discussed in Sec. III. Finally, a summary of our findings is presented in Sec. IV.

II. METHODOLOGY

The Su-Schrieffer-Heeger (SSH) model¹⁵ is the most commonly used theoretical model for describing carbon based π -conjugated systems. Here we have used an extended version of the SSH model which includes a three-dimensional description of the system based on internal coordinates (bond distances and bond angles^{13,16} as well as

^{a)}Electronic address: lingi@ifm.liu.se

^{b)}Electronic address: asajo@ifm.liu.se

^{c)}Electronic address: sst@ifm.liu.se

dihedral angles). Since the changes in the geometrical variables following excitations or charge transport are small, these changes can be approximated with linear terms for π -electron hopping and classical harmonic terms for the potential energy of the σ system. In order to keep a realistic geometry of the system it is also important to include the bond angles in the lattice potential. This is done by introducing a term in the lattice part of the Hamiltonian which takes the energy increase caused by deviations from the ideal geometry of a sp^2 structure into account. A similar term has also been included to account for the energy associated with changes in the dihedral angles. For the π system, however, the effect of these angles is very small. The hopping term that describes the energetics of the π system is therefore restricted to account for changes in the (nearest neighbor) bond lengths.

The SSH Hamiltonian with an additional term describing the external electric field has the form

$$H(t) = H_{el} + H_{\mathbf{E}} + H_{latt}$$

where the electronic part is defined as

$$H_{el} = - \sum_{\langle nn' \rangle} \hat{c}_n^\dagger t_{nn'} \hat{c}_{n'} = - \sum_{\langle nn' \rangle} \hat{c}_n^\dagger [t_0 - \alpha(r_{nn'} - a)] \hat{c}_{n'}. \quad (1)$$

All summations are over nearest neighboring carbon atoms, here denoted by $\langle nn' \rangle$, $t_{nn'}$ is the hopping integral between nearest neighbor carbon atom n and n' and t_0 is the hopping at a reference distance a . The actual interatomic distances are denoted by $r_{nn'} \equiv |\mathbf{r}_n - \mathbf{r}_{n'}|$ and α is the electron phonon coupling constant.

In the simulations which include an external electric field \mathbf{E} the following term has been added to the electronic part of the Hamiltonian,

$$H_{\mathbf{E}} = -e \sum_n \mathbf{r}_n \cdot \mathbf{E} (\hat{c}_n^\dagger \hat{c}_n - 1). \quad (2)$$

The field is constant both spatially and in time after a smooth turn on.¹⁴

The rest of the interactions in the system are described classically as:

$$\begin{aligned} \hat{H}_{latt} = & \frac{K_1}{2} \sum_{\langle nn' \rangle} (r_{nn'} - a)^2 + \frac{K_2}{2} \sum_n (\phi_n - \phi_0)^2 \\ & + \frac{K_3}{2} \sum_n (\theta_n - \theta_0)^2. \end{aligned}$$

Here K_1 , K_2 , and K_3 are harmonic spring constants accounting for σ -bond forces, ϕ_n denotes an angle in which atom n participates, and θ_n is a dihedral angle to which atom n contributes. All summations are over unique distances and angles to avoid double counting of these energy contributions. The angles ϕ_0 and θ_0 are those of the ‘‘relaxed’’ ground state geometry (see further below).

The equation of motion for the atoms is

$$M \ddot{\mathbf{r}}_n = - \nabla_{\mathbf{r}_n} \langle \Psi | H | \Psi \rangle, \quad (3)$$

where M is the mass of a CH-group (or a carbon atom in the case of C_{60}). The solution of the equation is

$$\begin{aligned} -M \ddot{q}_n^i(t) = & \sum_{\langle nn' \rangle} [K_1(r_{nn'} - a) + 2\alpha\rho_{nn'}] \frac{-(q_{n'}^i - q_n^i)}{r_{nn'}} \\ & - \sum_{\langle nn' \rangle} [t_0 - \alpha(r_{nn'} - a)] \frac{\partial \rho_{nn'}}{\partial q_n^i} \\ & + \sum_n K_2(\phi_n - \phi_0) \frac{\partial \phi_n}{\partial q_n^i} \\ & + \sum_n K_3(\theta_n - \theta_0) \frac{\partial \theta_n}{\partial q_n^i} - eE_i(\rho_{nn} - 1), \quad (4) \end{aligned}$$

where q_n^i with $i=1, 2$, and 3 indicate the x , y , and z coordinates of atom n , e is the electron charge, E_i is the x , y , or z component of the external electric field \mathbf{E} , and $\rho_{nn'}$ is an element in the density matrix. Since the system is close to its ground state configuration, the term which includes the derivative of the density with respect to a coordinate ($\partial \rho_{nn'} / \partial q_n^i$) is close to zero and therefore neglected in the numerical integration.

The elements of the density matrix $\rho_{nn'}(t)$ are calculated from

$$\rho_{nn'}(t) = \sum_k \psi_{nk}(t) f_k \psi_{n'k}^*(t), \quad (5)$$

where f_k is the time-independent distribution function being 0, 1, or 2 depending on initial state occupation and $\{\psi_k(t)\} = |\Psi(t)\rangle$ are the solutions to the time-dependent Schrödinger equation:

$$i\hbar |\dot{\Psi}(t)\rangle = (H_{el} + H_{\mathbf{E}}) |\Psi(t)\rangle. \quad (6)$$

In order to understand the behavior of the electron dynamics we introduce an expansion of these wave functions in a basis of instantaneous eigenfunctions, φ_k

$$\psi_k(t) = \sum_{k'} \varphi_{k'} \alpha_{k'k}(t),$$

where the instantaneous orbitals ($\{\varphi_k\} = |\varphi\rangle$) are obtained from the solution to the time-independent Schrödinger equation:

$$(H_{el} + H_{\mathbf{E}}) |\varphi\rangle = \epsilon |\varphi\rangle.$$

Transitions between the instantaneous eigenstates are made possible by the description in terms of the time-dependent equation, which is not possible for ‘‘adiabatic dynamics’’ with fixed level occupation. The time-dependent occupation number of the instantaneous eigenstate φ_k is given by¹⁷

$$n_k(t) = \sum_{k'} f_{k'} |\alpha_{k'k}(t)|^2. \quad (7)$$

This occupation number will be used to characterize the nature of the electronic relaxations in highly excited systems.

The values used for the parameters entering the equations introduced above can be found in Table I. The values

TABLE I. SSH parameter values for PPV and C_{60} .

Parameter/molecule	PPV	C_{60}
t_0 (eV)	2.66	1.91
α (eV/Å)	8.5	5.0
a (Å)	1.398	1.438
K_1 (eV/Å ²)	99.0	42.0
K_2 (eV/rad ²)	70.0	8.0 ^a /7.0 ^b
K_3 (eV/rad ²)	200.0	200.0
M [eV(as) ² /Å ²]	134 931 260 1.0	124 484 533 7.0

^afor a pentagon angle.^bfor a hexagon angle.

were partly obtained from Mizes and Conwell¹⁸ for the PPV and from You *et al.*¹⁶ for the C_{60} . Some parameters are new and others are altered in order to fit experimental values of the band gap and the bond distances. In principle, the parameter values should be different for different types of bonds in PPV.¹⁹ However, for simplicity the same values of t_0 and α were used for the different bonds in both PPV and C_{60} . Different spring constants K_n are used for the phenylene part and the single and double bonds in the vinylene part. The interaction between PPV-PPV and PPV- C_{60} is defined only via hopping, which is set to 0.1 eV (in PPV-PPV) and 0.2 eV (in PPV- C_{60}) between nearest neighbor sites on the two subsystems.

When optimizing the starting geometries of the molecules we minimized the total energy with respect to the atomic positions in all three dimensions, with the constraint to keep the molecular size constant, i.e., $\sum_{\langle nn' \rangle} (r_{nn'} - a) = 0$. For the optimization, the resilient propagation (RPROP) (Ref. 20) method was used.

The value of ϕ_0 was set to 120.0° for PPV. For C_{60} the pentagon angles were set to $\phi_0 = 108.0^\circ$ and the hexagon angles to $\phi_0 = 120.0^\circ$. These values are close to the *ab initio* HF 6-31G optimized values.¹⁴ The reference dihedral angle θ_0 was that of a planar PPV chain and, in the case of C_{60} , it was set to make the faces of the icosahedron planar. The exact values depend on the definition of a specific angle.

The atomic positions and the charge density were numerically integrated in time by solving the coupled differential equations, Eqs. (3) and (6) above. This is done using an eighth order Runge-Kutta integration with step-size control²¹ which in practice means a time step of less than 10 as. The “global time step” is 1 fs.

III. RESULTS

A. Single and multiple PPV systems

The simulations presented here describe the evolution of the PPV system following an excitation of the electronic system. The most relevant initial state geometry to use in this type of simulation is the equilibrium geometry of the ground state of the system. We will also discuss the effect of an initial state in which some lattice vibrations have been excited, which simulates the effect of a finite temperature.

The first system to study here is a single chain with 20 repeated units (158 carbon atoms). This is about the maximum conjugation lengths that can be achieved in a PPV

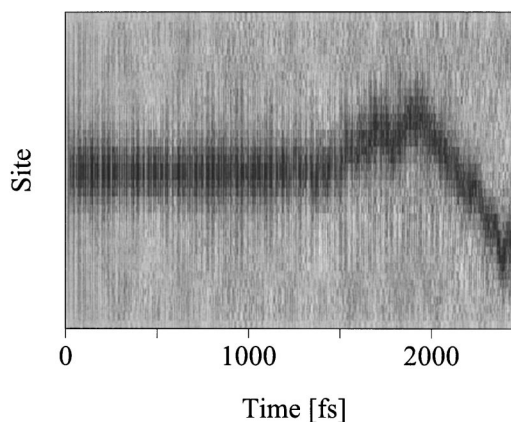


FIG. 1. Time evolution of the bond length order parameter for a 20 PPV unit long chain excited from HOMO to LUMO.

compound. The results from the simulation, in terms of the calculated changes in the bond lengths along the PPV chain as a function of time, are shown in Fig. 1. The simulation starts (at $t=0$) with a vertical electronic excitation from the highest occupied molecular orbital (HOMO) to LUMO. This excited state is delocalized over essentially the whole system. After ≈ 15 fs, the excited electron together with the hole in the HOMO level localize to the center of the chain and form a polaron exciton with a width of approximately four phenylene-vinylene repeat units. This extremely fast process has not been resolved experimentally, but it was concluded by Kersting *et al.*⁷ that the vibronic relaxations following an electron excitation are much faster than the sub-ps timescale which they could resolve. The dark region in the middle of the chain defines the region of the polaron exciton. The geometrical changes in this region correspond to a local contraction of the lattice. The excess energy which is released from the polaron exciton when it undergoes the rapid structural relaxation is transferred to local acoustic lattice vibrations that move up and down the polymer chain with the velocity of sound.

During a first period of about 1.5 ps essentially no movement of the polaron exciton is observed. There is, however, a considerable internal dynamics, the position of the electron and hole wave functions change from side to side of the lattice defect. The atoms within the region of the polaron exciton are also vibrating but these vibrations are trapped by the exciton²² and there is no collective movement of the defect. After ≈ 1.5 ps, however, the exciton suddenly starts to move along the chain with a velocity of ~ 0.2 Å/fs. As suggested by Onsager,²³ this motion follows a stocastical pattern, very similar to a Brownian type of motion and is caused by scattering of the polaron exciton by the phonons that exist outside the region of the exciton.

To further investigate the effect of these external phonons we let the chain contain some excess initial energy. This can be done in several ways, either by initially displacing individual atoms from their (neutral) ground state positions, and/or by giving the atoms initial velocities. Both these starting conditions will, after a few femtoseconds, result in more or less the same type of lattice excitation, namely a set of incoherent phonons simulating a nonzero initial tempera-

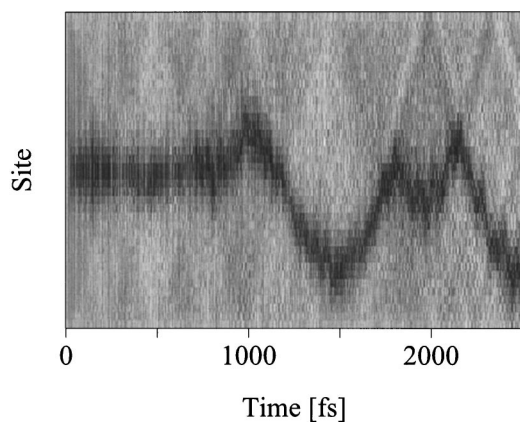


FIG. 2. Same as Fig. 1 but with extra lattice energy.

ture of the lattice. Here, the excess energy is introduced in the form of random initial displacements of the individual carbon atoms. The total excess energy which is added to the system in this way is 1 eV or about 6 meV per carbon atom. This extra energy causes the exciton to move within a shorter period of time after the excitation, in this case in ~ 900 fs. The bond length order parameter displayed in Fig. 2 shows a very clear picture of a random motion of the polaron exciton up and down the chain. It is also clear from this picture that the amplitudes of the lattice vibrations are much larger than in the previous case. Some of the vibrations are quite localized and originate from the region of the creation of the exciton. In our representation of the order parameter, the brighter regions correspond to an expanded segment of the polymer chain. These regions bounce back and forth over the chain with a speed of ≈ 0.24 Å/fs, which for parameter values used here corresponds to the sound velocity in the system.

We have also performed calculations for shorter chains. As one can expect, the polaron exciton starts to move faster in this case. The reason for this behavior is that the polaron exciton occupies a larger fraction of the chain and scattering by lattice vibrations therefore become more frequent.

Similar effects can be seen in a system where instead of moving one electron from the HOMO to LUMO we put an extra electron in the LUMO and in such a way we create an electron polaron. This situation corresponds to the case when an electron is injected into the polymer chain either from an electric contact or when the electron is hopping (under the influence of an external field) from a neighboring polymer chain. The polaron will behave in the same way as the exciton but the time span before it starts to move is much larger. In a simulation similar to that shown in Fig. 1 the scattering time out of the equilibrium position of the polaron in the middle of the chain is ~ 3 ps. This is natural since the excess energy associated with the extra electron is smaller than in the case of the HOMO to LUMO excitation, and there are therefore less phonons that can interact with the electron polaron.

If we take the next symmetric excitation, the HOMO-1 to LUMO+1 level, the exciton is more delocalized over the chain (see Fig. 3). There are two regions along the chain to which the exciton initially is localized. After ≈ 400 fs these

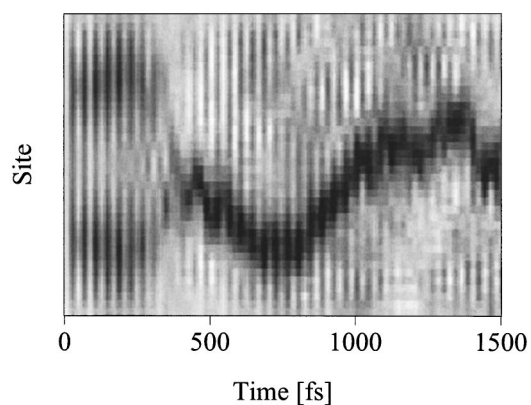


FIG. 3. Same as Fig. 1 but for a HOMO-1-LUMO+1 excitation.

two regions merge into one. This transition is associated with an electronic transition from LUMO+1 to LUMO of the excited electron and a corresponding transition of the hole from HOMO-1 to HOMO. If we go further and excite from HOMO-2 to LUMO+2 we get three regions in which the exciton initially exists. The excited state has a life time of about 150 fs before it relaxes into the HOMO to LUMO excited state. The initial shape of the exciton reflects the symmetry of the wave functions, which affect the geometry according to Eq. (5). The shorter life time of the exciton is a result of a lower energy barrier for scattering out of this state. The HOMO-3-LUMO+3 excitation first relaxes into the HOMO-1-LUMO+1 excitation, which takes about 100 fs, and then reach the final excitonic state of the HOMO-LUMO excitation.

The polaron exciton generated by the HOMO-1 to LUMO+1 excitation starts to move directly after this final transition (see Fig. 3). In this case, the energy released by the electron during the relaxation process generates enough phonons to scatter the polaron exciton and give it a nonzero velocity. Note that complete relaxation to the ground state is not allowed in our model due to symmetry restrictions. However, this dipole allowed transition is very slow, of the order of microseconds,²⁴ compared to the time scale of the relaxation processes studied here. (Some transitions between higher lying states are also only dipole allowed which might affect the relaxation process slightly.) However, we believe that our simulation gives a qualitatively correct description of the fast excitation dynamics of PPV.

Above we have discussed the relaxation process in terms of electronic relaxation and generation of lattice vibration, i.e., thermalization of hot excitations. The vibrations that couple most strongly to the electronic system are of course those that affect the bond lengths [see Eq. (5)], whereas bending modes do not enter explicitly this type of coupling. Quantitatively, we find most of the C-C stretching modes in bands around 1400 and 2400 cm^{-1} . The numerical values of these frequencies are, as in the case of the sound velocity discussed above, of course dependent on the parameters that are used in the Hamiltonian (see Table I). In our model we have not optimized these parameters to fit experimental data for these frequencies. Experimentally, these most predominant C-C stretching modes of PPV are found in bands

around 1330 and 1628 cm^{-1} .²⁵ The difference between our results and the experimental data is partially due to the fact that we do not include the hydrogen atoms explicitly. Therefore, any contribution to the vibrational modes coming from degrees of freedom associated with these atoms will be absent in our model. The effect of these errors in vibrational frequencies on the results of our simulations is difficult to estimate. Since the frequencies are too large in our model the energy stored in the lattice is also larger than in the real system. This indicates that the energy transfer from the electronic system, in the case of hot excitations, is too fast in our simulations.

In order to include the effect of inter chain interactions into our simulations we have performed studies on a system consisting of two identical PPV chains, both with a length of 20 repeat units. The two chains have an overlap of five repeat units and are electronically coupled to each other via a nearest neighbor interaction set to 0.1 eV.

The initial HOMO to LUMO excitation for the two chain system is distributed over both chains and localized to the region of the overlap. This localization reflects the spatial distribution of the HOMO and LUMO orbitals. After a very short time period, about 20 fs, the exciton is transferred to one chain but still localized to the overlap region. With two identical chains the localization to a single chain is arbitrary. Otherwise, with two chains of different length (20 and 16 repeat units in our simulation), the exciton appears on the longer chain. Similarly, when exciting from HOMO-1 to LUMO+1 we get an excitation localized to two different regions, one in the middle of each chain. After ~ 400 fs the excitation relaxes down to the HOMO-LUMO polaron exciton. In contrast to the case of a single chain, the energy of the lattice vibrations is not enough to scatter the exciton out of the potential well of the overlap in any of these two cases. We need an excitation from HOMO-2 to LUMO+2 to get enough excess lattice energy to create a mobile exciton.

B. Charge separation in PPV

In order to generate charge carriers by means of separation of the electron from the hole, we apply an external electric field to the PPV system. We use the double chain system in these studies since intrachain electron-hole separation is unrealistic.²⁶ The field is applied parallel to the chain direction and is turned on smoothly so that the maximal electric field is achieved within ≈ 80 fs.

The field is first applied to a system which has been excited from the HOMO to the LUMO level. From the studies presented above we know that this excitation will result in a polaron exciton. For a field strength of 2.8 $\text{mV}/\text{\AA}$ there is a nearly complete charge separation after ≈ 300 fs. The result of this simulation is shown in Fig. 4. As the field strength is increased, the delay time is reduced, for 3.5, 4.2, and 5.5 $\text{mV}/\text{\AA}$ it takes 200, 125, and 100 fs, respectively. This dependence on electrical field for photo conduction is in accordance with experimental results obtained^{27,28} (and predicted by Onsager²³). For lower field strength than 2.8 $\text{mV}/\text{\AA}$ there occurs no splitting within 2 ps. A direct comparison with experimental data is very difficult to make since there is no infor-

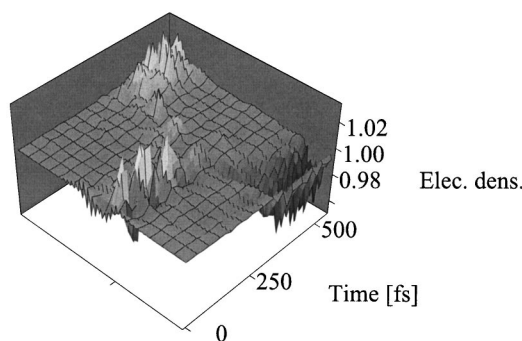


FIG. 4. Atomic charges in a system of two 20 unit long PPV chains excited from HOMO to LUMO with an electric field strength of 2.8 $\text{mV}/\text{\AA}$ applied along the chain direction. The sites along the two chains are displayed after each other on one of the horizontal axis.

mation concerning how the field is distributed over microscopic scales. It is clear, however, that there is a lower limit in the field strength for which dissociation can occur. Kersting *et al.*⁷ reported values of around 5 $\text{mV}/\text{\AA}$ in poly(phenylphenylenevinylene), which is in quite good agreement with the results of our simulation, whereas Khan *et al.*⁸ obtained a threshold value of around 10 $\text{mV}/\text{\AA}$ in MEH-PPV.

Again, it is very interesting to see how an increase in the initial lattice energy (higher temperatures) affects the charge separation time. We perform this study in the same way as above, we add an initial average lattice energy of 6 meV per atom (1 eV per chain) and then start the simulations. In Fig. 5 is shown how the charge separation is affected. The exciton dissociation occurs earlier for the system with more energy but the electron/hole ratio converges to a slightly lower value. This enhancing effect of temperature on photo conductivity has also been observed experimentally by, e.g., Frankevich *et al.*²⁹ It has also been discussed by Arkhipov *et al.*³⁰ that the vibrational heat bath contributes to the escape of the charges from the potential well formed by the superposition of the Coulomb and external field. An even more rapid charge separation is obtained by increasing the excitation energy [Fig. 5, curve (c)] to that of the HOMO-1 to LUMO+1 energy separation. In this case the charge separation occurs within 100 fs. It should be noted that the addi-

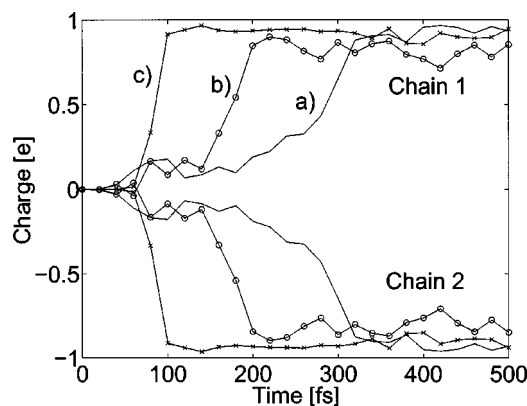


FIG. 5. Net charges (in units of $-|e|$) for the two chains with a 2.8 $\text{mV}/\text{\AA}$ field. (a) HOMO-LUMO excitation, (b) HOMO-LUMO excitation with 2 eV extra lattice energy per chain, and (c) HOMO-1-LUMO+1 excitation.

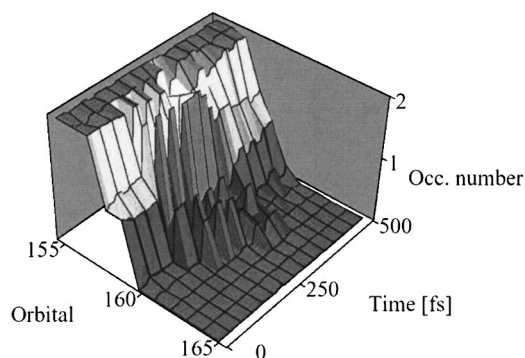


FIG. 6. The instantaneous occupation numbers for the simulation shown in Fig. 4.

tional total energy is smaller in this case than in the case of adding lattice energy. However, by affecting the electronic system directly, the energy barrier for charge separation is obviously much lower which explains the fast separation following the HOMO-1 to LUMO+1 excitation. This behavior has also been observed experimentally by Khan *et al.*⁸ who studied the fluorescence quenching in MEH-PPV as a function of excitation energy. They concluded that the threshold field strength for fluorescence quenching is lowered for higher excitation energies and that higher-energy excitons are more easily dissociated into electron-hole pairs by the field.

Using the time-dependent occupation number $n_k(t)$ introduced in Eq. (7) we can get information concerning the electronic degrees of freedom during the charge separation process. These occupation numbers are displayed in Fig. 6 as a function of time. As discussed above, $n_k(t)$ are obtained by projecting the solutions to the time-dependent Schrödinger equation onto the manifold of eigenstates obtained from a solution of the time-independent Schrödinger equation using the instantaneous atomic positions. At $t=0$, these occupation numbers are the expected, namely, single occupancy of the spin degenerate HOMO (orbital 158) and the LUMO (orbital 159) levels. During the time interval up to 150 fs, there is hardly any redistribution of the electrons among the different orbitals, which indicates that the dynamical behavior up to this point is an adiabatic process. During the period of charge separation, however, the electrons redistribute significantly, the hole moves from the HOMO to the HOMO-1 level and the electron is promoted to higher lying orbitals. The extra energy required for this redistribution comes from the external electric field. After the separation is completed, the electron distribution is again relaxed and corresponds approximately to the initial single occupancy of the HOMO and LUMO levels. Note, however, that these levels now are localized at the respective chain ends and not in the overlap region as initially. The very rapid electron-hole separation following the HOMO-1 to LUMO+1 excitation can be understood from this picture of charge separation since in that case, the system is already in the excited state which is required for this process to occur.

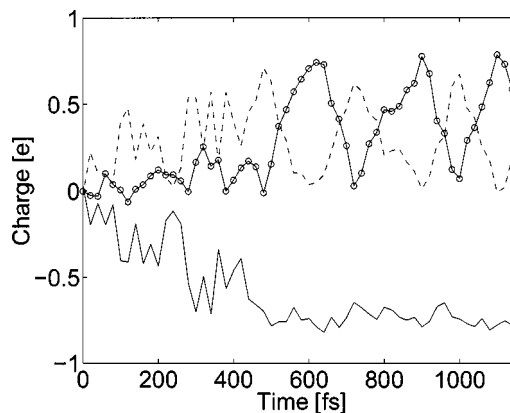


FIG. 7. Net charges (in units of $-|e|$) for the PPV- C_{60} system. The solid line shows the net charge on PPV, the dashed line C_{60} in contact with PPV, and the solid line with circles the second C_{60} molecule.

C. Charge separation in PPV C_{60}

One way to separate the exciton without an external electric field is to use an electron acceptor such as C_{60} .³ The C_{60} LUMO level lies below the LUMO of PPV. If the interaction between these two levels is sufficient it is possible that the exciton on a PPV chain disassociate and the electron moves onto the C_{60} with the hole left on the PPV chain.¹⁴ The systems we use consist of one PPV with 20 repeat units and one, two, or three C_{60} molecules. First we discuss the case of a single C_{60} molecule located at the middle of the PPV at a distance of 4 Å. Exciting an electron from HOMO to LUMO on the PPV chain leads to the creation of a polaron exciton (see above). Within a few integration time steps the LUMO level of PPV will start to hybridize with the C_{60} orbitals. Thus, the C_{60} molecule is affected within a very short period of time.⁵ However, the time for a complete charge separation is much longer. The relaxed system reaches maximum separation in approximately 1 ps. Similar to the simulations presented above we have added lattice energy to this system. This energy naturally lowers the barrier for charge separation but it also allows for the reverse reaction. The result in this case is that the polaron exciton moves back and forth between PPV and C_{60} . The extra energy in the system makes the hybridized levels move up and down which causes the electron to switch between the molecules which has the lowest LUMO level. Evidently, in the case of a system with only one C_{60} molecule, the system is too small for the charge carriers to be able to separate completely.

By introducing one or two additional C_{60} molecules the situation changes quite dramatically. The additional fullerenes are located in such a way that there is no contact between these molecules and the PPV chain. The time for the charge dissociation to occur can be seen in Fig. 7. The net charge on the C_{60} in contact with PPV is shown as the dashed line in the graph, the solid line showing positive charge represents the net charge on PPV. Evidently, charge separation starts immediately after the electronic excitation. After 100 fs there is a net positive charge of 0.4 μ charges on the PPV chain. This rapid process leads to induced vibrations on the C_{60} molecule, in agreement with experimental data.¹² This

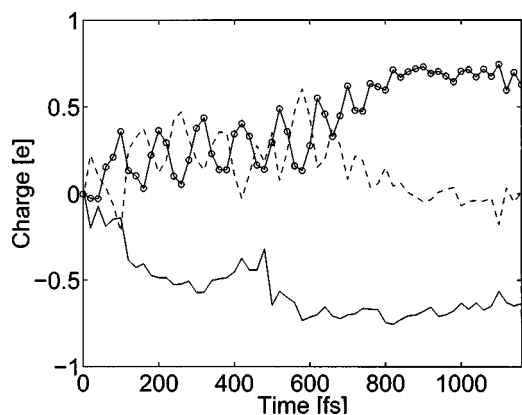


FIG. 8. Same as Fig. 7 but with a 2.8 mV/Å field applied perpendicular to the PPV chain axis.

net charge increases up to a maximum value of $\approx 0.8 \mu$ charges within 500 fs. After this charge separation process, the net charge on PPV remains essentially constant. The electron is transferred to the C_{60} dimer where it moves back and forth between the two molecules. In the case of a C_{60} trimer, the charge separation is even faster, ~ 300 fs. Consequently, we have shown that it is essential to have a concentration of C_{60} molecules in the vicinity of the PPV chain in order to separate the charges completely and within a relatively short period of time.

If we, in addition to the internal field between C_{60} and PPV, add an external electric field (possibly build up by using contacts with different Fermi energies) it is possible to move the charge along the C_{60} system. The field we used here was 4 mV/Å and aligned along the direction of C_{60} dimer which is perpendicular to the PPV chain axis. In Fig. 8 is shown the results of the same simulation as in Fig. 7 but with this external field included. The net charge on PPV increases with approximately the same rate as in the previous case but slightly more monotonically. Initially the electron transferred from PPV is shared between the two fullerene molecules, but after 700 fs the external field drives the electron to the C_{60} molecule located away from the PPV chain. Note that in none of the cases we have studied the charge transfer is complete, there is always some residual fractional charge of the electron left on PPV. This is a result of the hybridization and delocalization of the wave functions over the entire system. Again, if we go to larger systems, this effect will be smaller and full charge separation is expected in the macroscopic system.

IV. SUMMARY

An extended version of the SSH model which describes three dimensional structures has been applied to dynamical studies of excited systems including PPV and C_{60} . HOMO to LUMO electron excitation in PPV is followed by a very fast creation of a polaron exciton. The polaron exciton is initially located in the center of the PPV chain, but after about 1.5 ps it starts to move along the polymer chain. This motion is caused by scattering of the polaron exciton by localized lattice vibrations. By adding additional lattice energy to the system this scattering becomes more frequent and

the polaron exciton starts its motion within a shorter period of time after the excitation has occurred. We have also studied the dynamics following electron excitation to higher energy levels. In this case the electron relaxes down to the HOMO-LUMO excited state and a moving polaron exciton is created within 0.5 ps after the initial excitation.

In the second part of our work we study the dynamics of electron-hole (charge) separation in excited systems including PPV and C_{60} . In a system consisting of two coupled PPV chains separation depends crucially on the strength of the applied electric field. Below a field strength of 2.0 mV/Å we do not observe any charge separation whereas at 2.8 mV/Å charge separation occurs within 250 fs. The process of charge separation involves a redistribution of the electrons among the energy levels. This process is field induced but is also strongly dependent on the lattice energy (temperature) and the excitation energy. An increase in these two types of energies both lead to a shortening of the separation time.

In excited PPV and C_{60} , finally, the electron-hole separation is observed to occur spontaneously. The process starts immediately after excitation of PPV and is completed within ≈ 0.5 ps. The efficiency of this process depends crucially on the concentration of C_{60} molecules in the vicinity of the excited PPV chain.

With this quite detailed picture of the dynamical processes following electron excitation in PPV and C_{60} we hope that we can stimulate further improvement of the techniques to achieve charge separation in conjugated systems.

ACKNOWLEDGMENT

Financial support from the Swedish Research Council (VR) is gratefully acknowledged.

- ¹G. Yu, K. Pakbaz, and A. J. Heeger, *Appl. Phys. Lett.* **64**, 3422 (1994).
- ²J. H. Burroughes, D. D. C. Bradley, A. R. Brown, R. N. Marks, K. MacKay, R. H. Friend, P. L. Burns, and A. B. Holmes, *Nature (London)* **347**, 539 (1990).
- ³N. S. Sariciftci, L. Smilowitz, A. J. Heeger, and F. Wudl, *Science* **258**, 1474 (1992).
- ⁴S. Shaheen, C. Brabec, N. Sariciftci, F. Padinger, T. Fromherz, and J. Hummelen, *Appl. Phys. Lett.* **78**, 841 (2001).
- ⁵C. Brabec, N. S. Sariciftci, and J. Hummelen, *Adv. Funct. Mater.* **11**, 15 (2001).
- ⁶*The Nature of the Photoexcitations in Conjugated Polymers*, edited by N. S. Sariciftci (World Scientific, Singapore, 1997).
- ⁷R. Kersting, U. Lemmer, M. Deussen, H. J. Bakker, R. F. Mahrt, H. Kurz, V. I. Arkhipov, and H. Bässler, *Phys. Rev. Lett.* **73**, 1440 (1994).
- ⁸M. I. Khan, G. C. Bazan, and Z. D. Popovic, *Chem. Phys. Lett.* **298**, 309 (1998).
- ⁹W. Graupner, G. Cerullo, G. Lanzani, M. Nisoli, E. J. W. List, G. Leising, and S. De Silvestri, *Phys. Rev. Lett.* **81**, 3259 (1998).
- ¹⁰V. Gulbinas, R. Kananavicius, L. Valkunas, H. Bässler, and V. Sundström, *Mater. Sci. Forum* **384–385**, 279 (2002).
- ¹¹X. Wei, Z. N. Vardeny, N. S. Sariciftci, and A. J. Heeger, *Phys. Rev. B* **53**, 2187 (1996).
- ¹²V. Dyakonov, G. Zorinians, M. Scharber, C. J. Brabec, R. A. J. Janssen, J. C. Hummelen, and N. S. Sariciftci, *Phys. Rev. B* **59**, 8019 (1999).
- ¹³J. Bruening and B. Friedman, *J. Chem. Phys.* **106**, 9634 (1997).
- ¹⁴Å. Johansson and S. Stafström, *Phys. Rev. B* **68**, 035206 (2003).
- ¹⁵W. P. Su, J. R. Schrieffer, and A. J. Heeger, *Phys. Rev. B* **22**, 2099 (1980).
- ¹⁶W. You, C. Wang, F. Zhang, and Z. Su, *Phys. Rev. B* **47**, 4765 (1993).
- ¹⁷H. W. Streitwolf, *Phys. Rev. B* **58**, 14356 (1998).
- ¹⁸H. A. Mizes and E. M. Conwell, *Synth. Met.* **68**, 145 (1995).

- ¹⁹Z. Shuai, D. Beljonne, and J. Brédas, *Solid State Commun.* **78**, 477 (1991).
- ²⁰M. Riedmiller and H. Braum, in *Proceedings of the IEEE International Conference on Neural Networks* (San Francisco, CA, 1993), pp. 586–591.
- ²¹R. W. Brankinn, I. Gladwell, and L. F. Shampine, RKSUITE, Softreport 92-S1, Department of Mathematics, Southern Methodist University, Dallas, TX (1992).
- ²²A. J. Heeger, S. Kivelson, J. R. Schrieffer, and W. P. Su, *Mod. Phys. Lett. A* **60**, 781 (1988).
- ²³L. Onsager, *Phys. Rev.* **54**, 554 (1938).
- ²⁴J. Wang, Y. Lin, X. Hong, and M. El-Sayed, *Phys. Rev. B* **64**, 235413 (2001).
- ²⁵D. Rakovic, R. Kostic, L. A. Gribov, and I. E. Davidova, *Phys. Rev. B* **41**, 10744 (1990).
- ²⁶V. I. Arkhipov, E. V. Emelianova, S. Barth, and H. Bässler, *Phys. Rev. B* **61**, 8207 (2000).
- ²⁷D. Moses, J. Wang, G. Yu, and A. J. Heeger, *Phys. Rev. Lett.* **80**, 2685 (1998).
- ²⁸D. M. Pai and R. C. Enck, *Phys. Rev. B* **11**, 5163 (1975).
- ²⁹E. L. Frankevich, A. A. Lymarev, I. Sokolik, F. E. Karasz, S. Blumstengel, R. H. Baughman, and H. H. Hörhold, *Phys. Rev. B* **46**, 9320 (1992).
- ³⁰V. I. Arkhipov, E. V. Emelianova, and H. Bässler, *Phys. Rev. Lett.* **82**, 1321 (1999).